APH N.S., Heavy Ion Physics **13** (2001) 229–242

**HEAVY ION PHYSICS**
©Akadémiai Kiadó

# Phase Structure of the Semi-Classical Linear Sigma Model

Jørgen Randrup

Nuclear Science Division, Lawrence Berkeley National Laboratory
University of California, Berkeley, California 94720

*Received 12 December 2000*

**Abstract.** In order to establish a quantitative framework for assessing the reliability of dynamical simulations of DCC phenomena with the semi-classical mean-field treatment of the linear $\sigma$ model, we determine and discuss the phase structure implied by this approximate treatment. While the results appear to be physically reasonable for realistic scenarios, where the pion mass and the volume are finite, the approximate treatment might be less appropriate for idealized scenarios involving small masses and large volumes.

*Keywords:* Relativistic heavy-ion collisions, linear $\sigma$ model, phase structure.
*PACS:* 25.75.-q, 11.30.Rd, 11.10,-z, 11.15.Kc, 64.90.+b.

## 1. Introduction

Over the past several years, a considerable amount of research has been devoted to the prospect for exploring manifestations of chiral symmetry in high-energy nuclear collisions by means of the expected non-equilibrium dynamics during the expansion phase. The associated phenomena are often referred to as disoriented chiral condensates (DCC) and reviews of this topic can be found in Refs [1–3]. The environments produced in such collisions evolve rapidly in time and are spatially irregular, so it is necessary to base the treatment on microscopic dynamics and the appropriate tool would thus be real-time non-equilibrium quantum-field theory. Since such a treatment is beyond our current capabilities, the dynamical studies have been largely performed by means of classical field equations and by far the most popular framework has been the linear $\sigma$ model (for some examples, see Refs [4–13]).

A central goal of the high-energy nuclear collision effort is to extract information about the general phase properties of strongly interacting matter. However, it is no trivial task to infer the properties of matter in equilibrium (such as the equation of state) from the behavior of small systems that are out of equilibrium and rapidly changing. A consistent strategy would consist in seeking to reproduce the (observable) results of the collision dynamics by means of suitable microscopic simulations

1219-7580/01/ $ 5.00
©2001 Akadémiai Kiadó, Budapest

and then, once this has been achieved to a sufficient level of accuracy, infer the equilibrium properties of the physical system by applying the simulation treatment to a large system for a long time. For such an approach to be feasible, it is essential to know what equilibrium properties the adopted dynamical treatment actually yields. The implementation of this program is more problematic than might at first appear, because the need for having a tractable dynamical model usually requires that certain approximations be made in the treatment and, though possibly quite reasonable for the actual dynamical scenarios encountered, those approximations may be less appropriate in equilibrium.

The above general remarks apply in particular to the DCC studies. Within the linear $\sigma$ model, a variety of approximate treatments have been made. The most detailed and extensive dynamical simulations have been carried out by solving the classical field equation, with suitable initial conditions. The present investigation focuses specifically on the semi-classical treatment which initializes the quasiparticle modes of the field in accordance with quantum statistics [15]. We first give a condensed reminder of this particular treatment, which relies on a separation into order parameter and quasiparticle degrees of freedom, and we recall how it is possible to obtain expressions for the partition function and the associated free energy. With the framework set, we then move on to address the emerging phase structure for a range of physical scenarios specified by the value for the free pion mass and the volume of the system. We finally make a concluding discussion.

## 2. Semi-Classical Treatment of the Linear $\sigma$ Model

In its simplest form, applicable to baryon-free environments in which strangeness is ignored, the linear $\sigma$ model describes the degrees of freedom associated with the isoscalar $\sigma$ field and the isovector $\boldsymbol{\pi}$ field. For convenience those may be combined into an O(4) field $\boldsymbol{\phi}(\boldsymbol{r}) = (\sigma(\boldsymbol{r},t), \boldsymbol{\pi}(\boldsymbol{r},t))$. The Lagrangian density is then

$$\mathcal{L}(\boldsymbol{r},t) = \tfrac{1}{2}\partial_\nu \boldsymbol{\phi} \circ \partial^\nu \boldsymbol{\phi} - \tfrac{\lambda}{4}(\phi^2 - v^2)^2 + H\sigma \ , \tag{1}$$

where $\circ$ denotes the inner O(4) product and $\phi^2 = \boldsymbol{\phi} \circ \boldsymbol{\phi}$. The three model parameters, $\lambda$, $v$, and $H$, can be fixed by specifying the pion decay constant, $f_\pi$, the free pion mass, $m_\pi$, and the nominal $\sigma$ mass, $m_\sigma$. In vacuum, the field is aligned with the $\sigma$ direction, $\boldsymbol{\phi}_{\rm vac} = (f_\pi, \boldsymbol{0})$, and at low temperatures the agitations of the field represent nearly free $\sigma$ and $\pi$ mesons.

The present considerations are restricted to systems confined within a cubic box of volume $\Omega = L^3$; the continuum limit is then approached (rapidly) as $L \to \infty$. A given microscopic state of the system is characterized by the field $\boldsymbol{\phi}(\boldsymbol{r})$ and its time derivative $\boldsymbol{\psi}(\boldsymbol{r})$, both of which are real functions and have periodic boundary conditions. (The separate notation for the time derivative of the field emphasizes that it represents independent information and it is also notationally advantageous.) Once these quantities have been specified at a given time, their time evolution is determined by the associated equation of motion, which can be obtained by the usual variational procedure,

$$\left[\Box + \lambda(\phi^2 - v^2)\right] \boldsymbol{\phi} \;=\; H\hat{e}_\sigma \;. \tag{2}$$

This equation can be readily solved numerically (for example by employing the leap-frog propagation method on a Cartesian grid in position space).

It is useful to separate the field into two parts, $\boldsymbol{\phi}(\boldsymbol{r}) = \underline{\boldsymbol{\phi}} + \boldsymbol{\delta\phi}(\boldsymbol{r})$. The first part is the spatial average of the field, $\underline{\boldsymbol{\phi}} = \langle\boldsymbol{\phi}(\boldsymbol{r})\rangle$, and this quantity is identified with the O(4) order parameter associated with that particular field configuration. A similar decomposition can be made for the time derivative, $\boldsymbol{\psi}(\boldsymbol{r}) = \underline{\boldsymbol{\psi}} + \boldsymbol{\delta\psi}(\boldsymbol{r})$. The second part in the decomposition is the spatial fluctuation of the field and represents quasiparticle excitations relative to the uniform environment (or "false vacuum") characterized by the order parameter. The component of the field fluctuation $\boldsymbol{\delta\phi}$ (or its time derivative $\boldsymbol{\delta\psi}$) along the O(4) direction of the order parameter is denoted by $\delta\phi_\parallel$ (or $\delta\psi_\parallel$, respectively). The remainder is then perpendicular to $\underline{\boldsymbol{\phi}}$ and is denoted by $\boldsymbol{\delta\phi}_\perp$ (respectively $\boldsymbol{\delta\psi}_\perp$).

The separation of the field into order parameter and quasiparticle degrees of freedom provides a natural framework for linearizing the equation of motion (2). Employing a suitable Hartree factorization approximation, the linearization leads to a set of Klein–Gordon equations for the quasiparticle part, $\boldsymbol{\delta\phi}(\boldsymbol{r})$, and a separate equation of motion for the order parameter, $\underline{\boldsymbol{\phi}}$, with the equations being coupled via the respective effective masses [14]. The procedure is particularly simple to carry out in statistical equilibrium, as we shall now briefly recall.

### 2.1. Gap equations

When the quasiparticles are in (conditional) thermal equilibrium, their effective masses are determined by the given temperature, $T$, together with the magnitude of the order parameter, $\phi_0 = |\underline{\boldsymbol{\phi}}|$. To derive the associated gap equations, the first step is to take the spatial average of the equation of motion (2), thereby obtaining an equation of motion for the order parameter [16],

$$\left[\partial_t^2 + \mu_0^2\right] \underline{\boldsymbol{\phi}} = H\hat{\boldsymbol{e}}_\sigma \;. \tag{3}$$

The associated stiffness coefficient is given by

$$\mu_0^2 \;=\; \lambda[\phi_0^2 + \prec \delta\phi^2 \succ + \, 2 \prec \delta\phi_\parallel^2 \succ - \, v^2] \;, \tag{4}$$

where $\prec \delta\phi_\parallel^2 \succ$ denotes the thermal average of the field fluctuation along the O(4) direction of the order parameter $\underline{\boldsymbol{\phi}}$, while $\prec \delta\phi^2 \succ = \prec \delta\phi_\parallel^2 \succ + 3 \prec \delta\phi_\perp^2 \succ$ is the total field fluctuation (each of the three perpendicular fluctuation components have the same thermal average, $\prec \delta\phi_\perp^2 \succ$).

The above result can be used to understand the phase diagram, since the order parameter experiences no forces in equilibrium, $\partial_t^2\underline{\boldsymbol{\phi}} = \boldsymbol{0}$. Thus, at a given temperature $T$, the stationary points of $\underline{\boldsymbol{\phi}}$ are determined by $\mu_0^2\underline{\boldsymbol{\phi}} = H\hat{\boldsymbol{e}}_\sigma$, which implies that the equilibria are located on the $\sigma$ axis. If $\chi_0$ is the angle between $\underline{\boldsymbol{\phi}}$ and the $\sigma$ direction, the aligned component of the order parameter is given by $\sigma_0 = \phi_0 \cos\chi_0$ and the equilibrium condition then amounts to the relation $\mu_0^2\sigma_0 = H$. When the free pion mass vanishes, so does $H$. The condition for obtaining an equilibrium for a finite magnitude of the order parameter, $\phi_0 > 0$ (in which chiral symmetry is thus spontaneously broken), then amounts to the requirement that $\mu_0$ be zero.

However, in order to calculate the field fluctuations entering in $\mu_0^2$, it is necessary to know the quasiparticle masses. Subtracting the above equation of motion (3) from the complete equation (2) and applying a suitable Hartree factorization, approximate Klein–Gordon equations of motion can be obtained for the field fluctuations $\boldsymbol{\delta\phi}$ [15],

$$\left[\Box + \mu_\parallel^2\right] \delta\phi_\parallel = 0 \ , \quad \left[\Box + \mu_\perp^2\right] \boldsymbol{\delta\phi}_\perp = \mathbf{0} \ , \tag{5}$$

and the gap equations for the effective quasiparticle masses follow,

$$\mu_\parallel^2 \;=\; \lambda[3\phi_0^2 + \prec \delta\phi^2 \succ + \, 2 \prec \delta\phi_\parallel^2 \succ - \, v^2] \ , \tag{6}$$

$$\mu_\perp^2 \;=\; \lambda[\ \phi_0^2 + \prec \delta\phi^2 \succ + \, 2 \prec \delta\phi_\perp^2 \succ - \, v^2] \ . \tag{7}$$

We note that $\mu_0^2 \leq \mu_\perp^2 \leq \mu_\parallel^2$, with the equality signs holding for $\phi_0 = 0$. The quasiparticle energies are given by the corresponding Klein–Gordon dispersion relation, $(\omega_k^{(j)})^2 = k^2 + \mu_j^2$, where $j = \parallel, \perp$ denotes the particular O(4) component, and it is therefore now possible to express the thermal average of the field fluctuations,

$$\prec \delta\phi_j^2 \succ \;=\; \frac{1}{\Omega} \sum_{\mathbf{k}\neq\mathbf{0}} \frac{1}{\omega_k^{(j)}} \, \frac{1}{\mathrm{e}^{\omega_k^{(j)}/T} - 1} \ . \tag{8}$$

It is here important that the quasiparticle modes have been populated according to Bose–Einstein statistics.

In order to use the above result, it is necessary to find the self-consistent solution to the gap equations (6)–(7). For a given temperature $T$, a solution exists only if $\phi_0$ is sufficiently large. Since $\mu_\perp^2 \leq \mu_\parallel^2$, the associated critical boundary is determined by the vanishing of the transverse mass, $\mu_\perp = 0$. The critical boundary has a nearly parabolic form, starting out at $(v, 0)$ and ending at the *critical point* $(0, T_{\rm crit})$. Since all masses are degenerate for $\phi_0 = 0$, they all vanish at the critical point and the thermal fluctuation of each field component is then $T_{\rm crit}^2/12$). Consequently, the critical temperature is given by $T_{\rm crit}^2 = 2v^2$.

## *2.2. Partition function*

The discussion of the statistical properties of a system is most easily carried out on the basis of its partition function. Within the semi-classical treatment summarized above, it is fairly straightforward to calculate the associated partition function,

$$\mathcal{Z}_T \;=\; \int \mathcal{D}[\boldsymbol{\phi}(\boldsymbol{r}), \boldsymbol{\psi}(\boldsymbol{r})] \ \mathrm{e}^{-\frac{\Omega}{T} E[\boldsymbol{\phi}(\boldsymbol{r}), \boldsymbol{\psi}(\boldsymbol{r})]} \ . \tag{9}$$

A given microscopic state of the system specified by the value of the field at each point in space, $\boldsymbol{\phi}(\boldsymbol{r})$, together with the corresponding time derivative, $\boldsymbol{\psi}(\boldsymbol{r})$, and the functional integral is over all such field configurations. The statistical weight of a given field configuration is determined by its energy,

$$E[\boldsymbol{\phi}(\boldsymbol{r}),\boldsymbol{\psi}(\boldsymbol{r})] \;=\; \langle \tfrac{1}{2}\psi_0^2 + \tfrac{1}{2}(\nabla\phi)^2 + \tfrac{\lambda}{4}(\phi^2 - v^2)^2 - H\sigma\rangle \tag{10}$$

$$\;=\; E_0 + E_{\rm qp} + \delta V \;, \tag{11}$$

with $\psi_0 = |\underline{\boldsymbol{\psi}}|$. In the second line, this quantity has been decomposed into terms having instructive physical interpretations [15]. The first term in (11) is the energy density that would result if all the field fluctuations were put to zero,

$$E_0 \;=\; \tfrac{1}{2}\psi_0^2 \;+\; \tfrac{\lambda}{4}(\phi_0^2 - v^2)^2 \;-\; H\phi_0\cos\chi_0 \;. \tag{12}$$

It consists of the bare kinetic energy density $K_0 = \frac{1}{2}\psi_0^2$ and the bare interaction energy density $V_0$.

The second term in (11) is the energy associated with the gas of independent quasiparticles described by the above Klein–Gordon equations of motion (5),

$$E_{\rm qp} \;=\; \tfrac{1}{2}\langle \boldsymbol{\delta\psi}\circ\boldsymbol{\delta\psi} \;+\; \nabla\boldsymbol{\delta\phi}\circ\nabla\boldsymbol{\delta\phi} \;+\; \boldsymbol{\delta\phi}\circ\boldsymbol{M}\circ\boldsymbol{\delta\phi}\rangle \;, \tag{13}$$

where $\boldsymbol{M}$ is the quasiparticle mass tensor. In thermal equilibrium its major principal axis is oriented along the order parameter, the corresponding eigenvalue is $\mu_\parallel^2$, and the other three eigenvalues are equal to $\mu_\perp^2$.

The last term in (11) corrects for the fact that the interaction is non-linear,

$$\delta V \;=\; \tfrac{\lambda}{4}\langle\delta\phi^4\rangle - \tfrac{\lambda}{2}\langle\delta\phi^4\rangle_G \;\approx\; -\tfrac{\lambda}{4}\langle\delta\phi^4\rangle_G \tag{14}$$

$$\;=\; \langle\delta\phi^2\rangle^2 \;+\; 2\,{\rm Tr}(\langle\boldsymbol{\delta\phi\delta\phi}\rangle\circ\langle\boldsymbol{\delta\phi\delta\phi}\rangle) \tag{15}$$

$$\;\approx\; -\tfrac{3}{4}\lambda\,[\prec\delta\phi_\parallel^2\succ^2 + 2\prec\delta\phi_\parallel^2\succ\prec\delta\phi_\perp^2\succ \;+\; 5\prec\delta\phi_\perp^2\succ^2] \;\equiv\; \delta V_T \tag{16}$$

Here $\langle\cdot\rangle_G$ denotes the Gaussian approximation to the evaluation of the average. The last line arises if the spatial averages are approximated by the corresponding thermal averages, as is expected to be accurate when $L$ exceeds the correlation length. The resulting quantity, $\delta V_T$, then depends on the particular state only through the magnitude of its order parameter, $\phi_0$. It should be recognized that $\delta V$ is not negligible.

With the above preparations, we are now in a position to simplify the expression (9) for the partition function. We first note that the functional integral factorizes into a regular (8-dimensional) integral over the O(4) order parameter $\underline{\boldsymbol{\phi}}$ and its time derivative $\underline{\boldsymbol{\psi}}$ and a functional integral over the field fluctuation $\boldsymbol{\delta\phi}(\boldsymbol{r})$ and its time derivative $\boldsymbol{\delta\psi}(\boldsymbol{r})$,

$$\mathcal{Z}_T \;=\; \int d^4\underline{\boldsymbol{\psi}}\;{\rm e}^{-\frac{\Omega}{T}K_0}\int d^4\underline{\boldsymbol{\phi}}\;{\rm e}^{-\frac{\Omega}{T}(V_0+\delta V_T)}\int\mathcal{D}[\boldsymbol{\delta\phi}(\boldsymbol{r}),\boldsymbol{\delta\psi}(\boldsymbol{r})]\;{\rm e}^{-\frac{\Omega}{T}E_{\rm qp}}\;. \tag{17}$$

The integration over $\underline{\boldsymbol{\psi}}$ yields the factor $(2\pi T/\Omega)^2$, which may henceforth be neglected since it depends only on temperature. The integral over the quasiparticle degrees of freedom yields the conditional quasiparticle partition function $\mathcal{Z}_{\rm qp}$. We may write $\ln\mathcal{Z}_{\rm qp}=\ln\mathcal{Z}_{\rm qp}^{\parallel}+3\ln\mathcal{Z}_{\rm qp}^{\perp}$, where

$$\begin{aligned}
\ln\mathcal{Z}_{\rm qp}^{(j)} &= -\sum_{\mathbf{k}\neq\mathbf{0}}\ln[1-{\rm e}^{-\omega_k^{(j)}/T}] && (18)\\
&= \frac{1}{T}\sum_{\mathbf{k}\neq\mathbf{0}}\omega_k^{(j)}f_k^{(j)}-\sum_{\mathbf{k}\neq\mathbf{0}}[\bar{f}_k^{(j)}\ln\bar{f}_k^{(j)}-f_k^{(j)}\ln f_k^{(j)}] && (19)\\
&= \frac{\Omega}{T}(V_{\rm qp}^{(j)}-TS_{\rm qp}^{(j)})\ , && (20)
\end{aligned}$$

for each chiral component $j$, with $\bar{f}_k^{(j)}=1+f_k^{(j)}$. The total energy density of the quasiparticles is then $V_{\rm qp}=V_{\rm qp}^{\parallel}+3V_{\rm qp}^{\perp}$ and their entropy density is $S_T=S_{\rm qp}^{\parallel}+3S_{\rm qp}^{\perp}$. Consequently, we may write the overall partition function on a simple form,

$$\mathcal{Z}_T\ =\ \int d^4\underline{\boldsymbol{\phi}}\ {\rm e}^{-\frac{\Omega}{T}F_T}\ =\ \int d^4\underline{\boldsymbol{\phi}}\ {\rm e}^{-\frac{\Omega}{T}[V_T(\phi_0,\chi_0)-TS_T(\phi_0)]}\ . \tag{21}$$

Here free energy density is $F_T=V_T(\phi_0,\chi_0)-TS_T(\phi_0)$, with the effective potential energy density being $V_T=V_0(\phi_0,\chi_0)+V_{\rm qp}(\phi_0)+\delta V_T(\phi_0)$, so we have explicitly

$$\begin{aligned}
F_T &= \tfrac{1}{4}\lambda(\phi_0^2-v^2)^2\ -\ H\phi_0\cos\chi_0\\
&+ \frac{T}{\Omega}\sum\nolimits'_{\mathbf{k}}[\ln(1-{\rm e}^{-\epsilon_k^{\parallel}/T})+3\ln(1-{\rm e}^{-\epsilon_k^{\perp}/T})]\\
&- \tfrac{3}{4}\lambda\ [\prec\delta\phi_{\parallel}^2\succ^2\ +2\prec\delta\phi_{\parallel}^2\succ\prec\delta\phi_{\perp}^2\succ\ +5\prec\delta\phi_{\perp}^2\succ^2]\ .
\end{aligned} \tag{22}$$

It should be noted that the effective masses $\mu_\parallel$ and $\mu_\perp$, as well as the associated thermal field fluctuations $\prec\delta\phi_\parallel^2\succ$ and $\prec\delta\phi_\perp^2\succ$, are independent of the misalignment angle $\chi_0$. Thus the $\chi_0$ dependence of the free energy is only through the term $-H\phi_0\cos\chi_0=-H\sigma_0$ in the bare potential $V_0$. For $H>0$ this term has its minimum value for $\chi_0=0$ and it increases steadily until reaching its maximum for $\chi_0=\pi$. All stationary points of $F_T$ are therefore located on the $\sigma$ axis and occur where $(\partial F_T/\partial\sigma_0)_T$ vanishes.

## 3. Phase Structure

Once the expression for the partition function has been derived, it is possible to investigate the statistical properties of the chiral order parameter $\underline{\boldsymbol{\phi}}$. The equilibrium points can be identified as those where the free energy density $F_T$ is stationary. Using the expression for the free energy derived above, together with the self-consistent dispersion relations, it is elementary to show the following relation,

$$\left(\frac{\partial F_T}{\partial\sigma_0}\right)_T\ =\ \mu_0^2\ \sigma_0-H\ . \tag{23}$$

Since the right-hand side is recognized as the acceleration of the order parameter as given in Eq. (3), which must vanish at the equilibrium point, it follows that the statistical and dynamical equilibrium criteria are indeed identical, so the thermodynamic consistency of the treatment is ensured.

### *3.1. Idealized case*

Let us first consider the idealized case where $L \to \infty$ and $m_\pi = 0$. The former condition corresponds to the thermodynamic limit while the latter ensures perfect O(4) symmetry. Though both idealizations are quite unrealistic, this case is the most studied one and it may therefore provide a useful reference. The corresponding structure of the free energy density is illustrated in Fig. 1 and the resulting equilibria are traced out in Fig. 2.

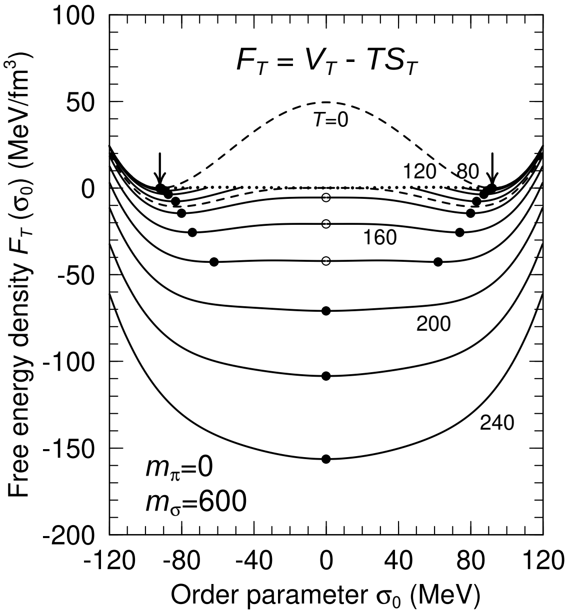


**Fig. 1.** The free energy density $F_T$ calculated with the semi-classical mean-field approximation to the linear $\sigma$ model, as a function of the order parameter $\sigma_0$ for various values temperatures $T$, for the idealized O(4) symmetric case ($m_\pi = 0$). At each $T$, the solid (or open) dots indicate the favored (or unfavored) equilibria. For $T < T_{\rm crit} = \sqrt{2}v$, the order parameter must exceed a certain minimum value before all quasiparticle modes are stable; the corresponding end points are connected by the dotted curve. The top dashed curve is the bare potential $V_0$ obtained for $T = 0$.

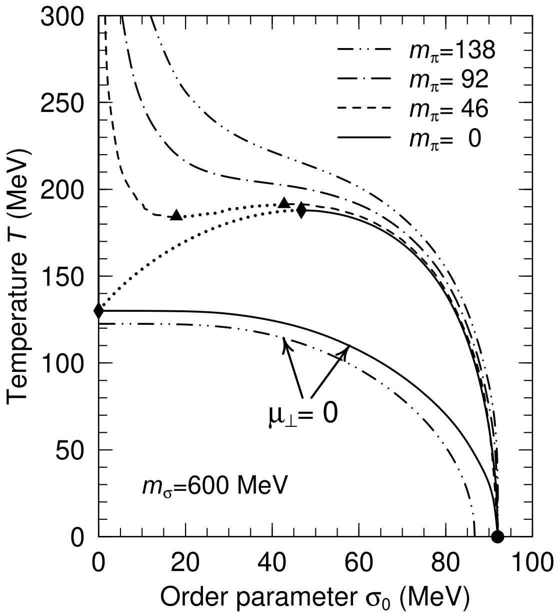


**Fig. 2.** The stable and unstable (dotted) equilibrium values of the chiral order parameter $\sigma_0 = \phi_0 \cos\chi_0$ at a given quasiparticle temperature $T$, as traced on the chiral phase diagram for the indicated four values of the pion mass $m_\pi$. For $m_\pi = 0$ the high-temperature O(4) symmetric equilibrium branch extends upwards along the vertical axis from the critical point marked by the diamond. The critical boundary defined by $\mu_\perp = 0$ (within which the field is supercritical) is delineated for $m_\pi = 0$ and 138 MeV/$c^2$. The solid dot is located at the common ground state, $\sigma_0 = f_\pi = 92$ MeV.

When the pion mass vanishes the ground-state minimum is located at $\sigma_0 = f_\pi$, where $F_T$ vanishes, $F_T^{\rm vac} = 0$. The minimum in $F_T$ moves inwards as $T$ is increased, at first very slowly and then progressively faster, until a certain temperature is reached, $T = T_{\rm tran}$. At this point the stationary points in $F_T$ turn from minima to maxima as the tracing curve continues downwards towards the critical point.

Once the temperature exceeds the critical value $T_{\rm crit}$, a solution to the gap equations exist for all values of $\phi_0$. From this temperature and up, the free energy has a minimum at $\phi_0 = 0$. Thus, in the temperature range between $T_{\rm crit}$ and $T_{\rm tran}$, there are two minima in $F_T$, separated by a maximum that is only slightly higher than the symmetric minimum. The outer minimum generally carries a larger statistical weight (the value of $F_T$ is lower). Consequently, it represents the thermodynamically preferred state and the symmetric configuration is merely metastable (with the maximum representing an unstable equilibrium). We therefore refer to $T_{\rm tran}$ as the *transition temperature*. Above $T_{\rm tran}$ there is only the symmetric minimum and the system then prefers chirally symmetric configurations.

This general structure of the free energy implies that the system will display a first-order phase transition at $T = T_{\rm tran}$, with the preferred magnitude of the order parameter dropping abruptly from a fairly large finite value to zero. However, as is evident from Fig. 1, the metastable minimum at $\phi_0 = 0$ is very shallow and a finite system would therefore display large fluctuations in $\phi_0$. To illustrate these features quantitatively, we note that at $T_{\rm crit}$ ($\approx$ 130 MeV), the free energy density at the inner minimum (the critical point) is close to zero,

$$F_T^{\rm crit} \;=\; (\frac{\lambda}{12} - \frac{8}{45}\pi^2) f_\pi^4 \;\approx 0.1642 \text{ MeV fm}^{-3} \;, \tag{24}$$

whereas it is $F_T \approx -10.6$ MeV fm$^{-3}$ at the outer minimum. Moreover, at the transition temperature $T_{\rm tran}$ ($\approx$ 188 MeV), the common value is $F_T \approx -50$ MeV fm$^{-3}$.

### *3.2. Finite mass*

Since the quark masses are in fact finite, chiral symmetry is only approximate in the real world and it is of interest to examine how the phase structure evolves as the pion mass is increased from the idealized value of zero towards its realistic mass $m_\pi \approx 138$ MeV. In Fig. 2 the equilibrium points are traced out in the phase diagram for four different values of $m_\pi$. As the pion mass is increased from zero, the phase structure described above will be gradually eroded, as the free-energy curves, $F_T(\sigma_0)$, will be tilted ever more strongly towards the positive $\sigma$ direction. As a result, all stationary points will be situated on the $\sigma$ axis, with the outer minimum occurring at $\sigma_0 = f_\pi$, while there will be a saddle point situated approximately oppositely. When the value of $m_\pi$ exceeds about half the physical value, the resulting tilting suffices to overpower the symmetric minimum altogether and there is then only a single minimum at any temperature (located on the positive part of the $\sigma$ axis). From that value on, the system displays a smooth crossover from a strongly broken to a weakly broken phase, with the most rapid change in order parameter occurring at temperatures somewhat above 200 MeV.

The phase structure discussed above is reflected in the behavior of the equilibrium values of the effective quasiparticle masses, as shown in Fig. 3. When the specified value of $m_\pi$ is sufficiently small, the associated phase transition causes a backbend in the mass curves, as the system is traced through the unstable equilibrium branch. For perfect O(4) symmetry ($m_\pi = 0$), the backbend reaches all the way to the critical point where all the effective masses vanish, $\mu_0 = \mu_\perp = \mu_\parallel = 0$, and from there on they are exactly degenerate and grow approximately linearly with $T$. As noted above, the branch with the large masses is generally the thermodynamically preferred one. For the case of $m_\pi = 0$, Fig. 3 also shows the evolution of $\mu_\parallel$ along the critical path where $\mu_\perp$ vanishes. It drops approximately quadratically from its free value at $T = 0$ to zero at $T_{\rm crit}$.

For the larger values of $m_\pi$, the evolution is smooth, but a remnant of the basic two-phase structure of the system remains visible as a distinct minimum in the $\sigma$ mass. The location of this minimum may be used as an indicator for the

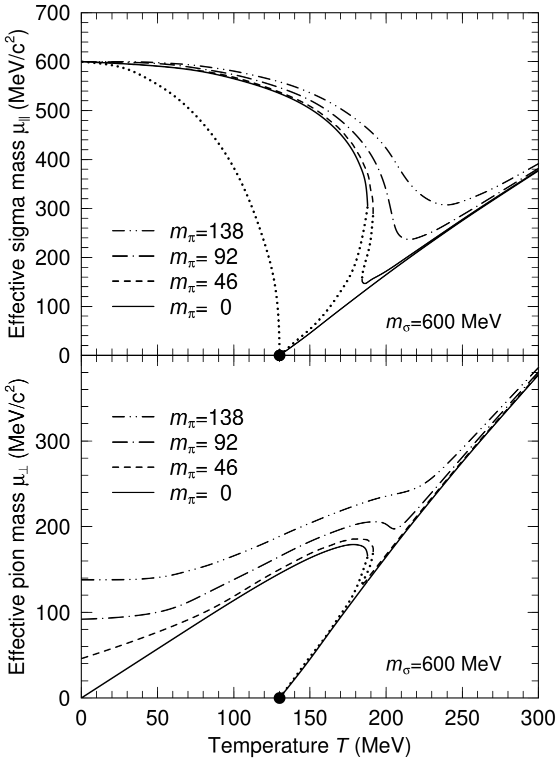


**Fig. 3.** The equilibrium values of the effective masses $\mu_\parallel$ (top) and $\mu_\perp$ (bottom) for $\sigma$-like and $\pi$-like quasiparticles, respectively, as functions of the temperature $T$, for the four different pion masses $m_\pi$ considered in Fig. 2; the values at the unstable equilibria are traced by the dotted curves. In addition, the top panel shows the value of $\mu_\parallel$ along the critical boundary for $m_\pi = 0$ (dotted curve on far left).

effective transition temperature [17]. At higher temperatures, the masses become nearly degenerate (and approximately proportional to $T$) as chiral symmetry is approached (the order parameter $\sigma_0$ then tends to zero as $\sim T^{-2}$).

### *3.3. Finite size*

Since the systems available for actual experimental study have a rather limited spatial extension, it is important to assess the importance of finite-size effects. As it turns out [15], the free energy density $F_T$ depends very little on the actual volume $\Omega$, once the side length $L$ is above 5 fm or so, and it makes no practical difference whether it is calculated in terms of the quantized modes, as indicated above, or in the continuum limit. Thus the size dependence of the statistical properties arises primarily through the volume $\Omega$ multiplying $F_T$ in the integrand in (21).

When the volume is small, the integrand in the partition function is no longer narrowly peaked at the minima in $F_T$. Rather, it represents a probability density in the O(4) space of the order parameter $\underline{\phi}$. Since $F_T$ depends only on the magnitude of the order parameter, $\phi_0$, and its angle of disorientation, $\chi_0$, it is instructive to project onto the plane of those two state variables [15],

$$\mathcal{Z}_T \;=\; \int_0^\infty d\phi_0 \int_0^\pi d\chi_0 \; W_T(\phi_0, \chi_0) \;, \tag{25}$$

where $W_T$ is the statistical weight for finding the system with an order parameter having the specified magnitude and misalignment,

$$W_T(\phi_0, \chi_0) \;=\; 4\pi\phi_0^3 \; \sin^2\chi_0 \; \mathrm{e}^{-\frac{\Omega}{T} F_T(\phi_0, \chi_0)} \;. \tag{26}$$

Generally speaking, the statistical fluctuations in a finite system tend to wash out the sharp structure characteristic of infinite matter. The importance of this effect on the temperature dependence of the order parameter is brought out in Fig. 4. The changes are most significant in the idealized O(4) symmetric scenario. In particular, it can be seen that the first-order transition obtained for $m_\pi$=0 becomes less prominent as the volume is decreased to realistic sizes and it has disappeared altogether for the smallest volume considered ($L \approx 5$ fm).

It is important to note that such qualitative change does not occur when a realistic value of $m_\pi$ is employed, since the behavior is then already smooth for large systems. In fact, the finite-size effect is hardly visible until rather small volumes are reached. Furthermore, for such small volumes the difference between the results obtained for the various specified values of $m_\pi$ is less noticeable. This feature suggests that a quantitative extraction of the matter equation of state from analysis of the small finite systems involved in actual experiments depends heavily on the availability of models that are quantitatively reliable.

### *3.4. Dynamical tests*

The statistical analysis underlying the above results invokes the Hartree factorization to obtain an effective-mass description of the quasiparticle modes. In order to gain an impression of how accurate this treatment is with regard to its predictions of the phase structure, a number of dynamical tests have been performed alongside the statistical analysis, in a manner similar to what was done already in Ref. [15].

For these dynamical tests, the classical field is prepared with its order parameter equal to a specified value and with the field fluctuations picked from the associated conditional equilibrium ensemble, according to the sampling method developed in Ref. [15]. For example, the system was prepared to be situated in the neighborhood of a predicted stable equilibrium point and its dynamical evolution was then determined by solving the full non-linear equation of motion (2). It was verified that

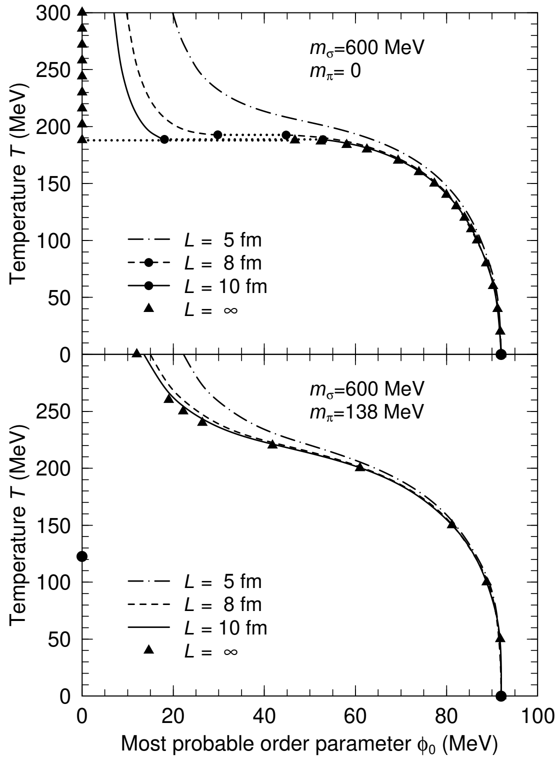


**Fig. 4.** The most probable value of the magnitude of order parameter, $\phi_0$, as a function of the temperature $T$, for various values of the side length $L$ of the cubic volume considered, with either $m_\pi = 0$ (top) or $m_\pi = 138$ MeV (bottom).

the order parameter would then start executing a damped oscillation around the predicted equilibrium point. Similarly, for a predicted unstable equilibrium point, it was checked that the order parameter would be repelled if the system were prepared in a nearby configuration. Furthermore, if the system was prepared at or near a metastable equilibrium point, the thermal fluctuations in the finite system would eventually lead to an ejection of the order parameter from the metastable basin and the system would approach the predicted global equilibrium point. From such dynamical tests, it appears that the presented statistical analysis in fact provides a quite reliable picture of the phase structure implied by the dynamical treatment.

It is important that such dynamical tests be carried out with suitable care. In particular, if the classical field propagation is carried too far in time, the inherent Rayleigh–Jeans problem may manifest itself, as the system will drift away from the semi-classical equilibrium neighborhood and approach a classical equilibrium corresponding to energy equipartition among the modes included in the numerical treatment. Fortunately for the practical applications to DCC phenomena, the associated relaxation time is significantly larger than the typical time needed for achieving a full decoupling of the modes, due to the rapid expansion and cooling.

## 4. Discussion

In the present work, we have studied the phase structure emerging with the semi-classical treatment of the simple linear $\sigma$ model. Starting from the canonical partition function, we have obtained the statistical weight as a function of the magnitude and orientation of the chiral order parameter. This has enabled us to determine the phase diagram for any given size of the volume, $\Omega$ and the free pion mass, $m_\pi$.

Relative to the much studied but quite unrealistic case of an infinitely large volume and a vanishing mass, we have examined the effects caused by the introduction of a finite pion mass and a finite value of the volume. While the idealized scenario of vanishing pion mass and infinite volume yields a first-order phase transition, this structure is gradually being eroded as either the mass or the volume is changed to more realistic values, and it is ultimately being replaced by a smooth crossover.

It has also been explicitly checked that the unapproximated field equation of motion (2), with the semi-classical initialization of the field, in fact leads to dynamical evolutions in accordance with the phase structure derived from the analysis of the calculated partition function. Thus the present results provide a good quantitative guide for what can be expected from dynamical simulations with this model.

Since it is expected on rather general grounds that a proper quantal treatment of the idealized O(4) symmetric case, in the thermodynamic limit, should yield a phase transition of second-order only [18], one should obviously be cautious about employing the present treatment to that case. Fortunately, this possible limitation has little bearing on the practical applications of the treatment to problems in high-energy collision dynamics, where the magnitude of the actual pion mass and the finite size of the systems both ensure a crossover behavior. Furthermore, since the scenarios of interest are rapidly expanding, a complete mode decoupling occurs relatively quickly and thus prevents the approach to equilibrium from proceeding very far. Therefore it appears that the semi-classical model may in fact provide a physically reasonable treatment of the problem, within the overall limitations arising from the neglect of specific quantum-field effects and additional degrees of freedom, such as strangeness or baryons.

In general, it is important to understand the phase properties implied by dynamical models being used in attempts to infer equilibrium properties of infinite systems from rapidly evolving small systems out of equilibrium. With this as our motivation, we have examined the semi-classical linear $\sigma$ model and sought to elucidate its phase structure for a range of physical scenarios. We expect that the results may be useful for assessing the physical utility of specific dynamical simulations with that model.

## Acknowledgments

The author is pleased to acknowledge helpful discussions with T. Hatsuda, J.I. Kapusta, E. Mottola and W. Weise. This work was supported in part by the Director, Office of Energy Research, Office of High Energy and Nuclear Physics, Nuclear Physics Division of the U.S. Department of Energy under Contract No. DE-AC03-76SF00098.

## References

1. K. Rajagopal, in *Quark-Gluon Plasma 2*, ed. R. Hwa, World Scientific, 1995.
2. J.-P. Blaizot and A. Krzywicki, *Acta Phys. Polon.* **B27** (1996) 1687.
3. J.D. Bjorken, *Acta Phys. Polon.* **B28** (1997) 2773.
4. K. Rajagopal and F. Wilczek, *Nucl. Phys.* **B404** (1993) 577.
5. M. Asakawa, Z. Huang and X.-N. Wang, *Phys. Rev. Lett.* **74** (1995) 3126.
6. L.P. Csernai and I.N. Mishustin, *Phys. Rev. Lett.* **74** (1995) 5005.
7. J. Randrup, *Phys. Rev. Lett.* **77** (1996) 1226.
8. G. Amelino-Camelia, J.D. Bjorken, and S.E. Larsson, *Phys. Rev.* **D56** (1997) 6942.
9. A. Abada and M.C. Birse, *Phys. Rev.* **D57** (1998) 292.
10. A.K. Chaudhuri, *Phys. Rev.* **D59** (1999) 117503.
11. D. Kaiser, *Phys. Rev.* **D59** (1999) 117901.
12. T.C. Petersen and J. Randrup, *Phys. Rev.* **C61** (2000) 024906.
13. Z. Xu and C. Greiner, *Phys. Rev.* **D62** (2000) 036012.
14. J. Randrup, *Nucl. Phys.* **A616** (1997) 531.
15. J. Randrup, *Phys. Rev.* **D55** (1997) 1188.
16. G. Baym and G. Grinstein, *Phys. Rev.* **D15** (1977) 2897.
17. R.D. Pisarski, *Phys. Rev.* **D52** (1995) R3773.
18. See, for example, J. Cardy, *Scaling and Renormalization in Statistical Physics*, Cambridge University Press, 1996.